Biochemistry

 Volume 20, Number 6 March 17, 1981

# Thermodynamics of $(dG–dC)_3$ Double-Helix Formation in Water and Deuterium Oxide†

Diane DePrisco Albergo, Luis A. Marky, Kenneth J. Breslauer, and Douglas H. Turner*

ABSTRACT: The thermodynamics of double-helix formation by $(dG\text{-}dC)_3$ in $H_2O$ and $D_2O$ were measured spectrophotometrically and calorimetrically. Spectrophotometric values based on plots of inverse melting temperature vs. log of concentration are in good agreement with calorimetry. However, spectrophotometric values based on the shape of absorbance vs. temperature curves are in good agreement with calorimetry only if linear pre- and posttransition base lines are subtracted before analysis. The averages of the enthalpies measured by the three most reliable spectroscopic methods are −56.9 and −62.7 kcal/mol of helix in $H_2O$ and $D_2O$, respectively. The corresponding calorimetric values are −59.6 and −65.8 kcal/mol of helix.

Knowledge of the thermodynamics of double-helix formation by oligonucleotides is important for predicting secondary structure in nucleic acids and for understanding the forces directing nucleic acid chemistry (Borer et al., 1974; Gralla & Crothers, 1973; Pohl, 1974; Albergo & Turner, 1981). With one exception, all the available thermodynamics have been obtained from melting curves measured spectrophotometrically. Unfortunately, the final values depend on the model assumed and the analysis employed. For example, the enthalpy derived by using a two-state model for the helix to coil transition will depend on whether the experimentally measured parameter is the slope of the melting curves at the melting temperature ($T_m$) or the slope of a plot of $1/T_m$ vs. the log of concentration. The one oligomer studied nonspectrophotometrically is $rA_7U_7$ (Breslauer et al., 1975). In that study, the enthalpy determined calorimetrically was compared with that derived from various optical methods. This paper presents a similar comparison for $(dG\text{-}dC)_3$ in both $H_2O$ and $D_2O$ under conditions where it forms a right-handed double helix (Albergo & Turner, 1981). Despite the major differences between $(dG\text{-}dC)_3$ and $rA_7U_7$, both studies indicate that enthalpies derived from $1/T_m$ vs. the log of concentration plots agree well with calorimetric values. This is an important result since spectrophotometric measurements require less material, use readily available instrumentation, and are therefore easier to perform.

## Experimental Procedures

*Oligonucleotide.* d-GpCpGpCpGpC was purchased from Collaborative Research, and purity was checked by high-pressure liquid chromatography on a 25-cm $C_{18}$ reverse-phase column with 10-μm particle size. A linear gradient was run from 2 to 14% acetonitrile in aqueous buffer containing 0.05 M $(NH_4)_2HPO_4$ and 0.05 M $NaH_2PO_4$, pH 7.0. A single symmetric peak was observed. When coinjected with a sample of $(dG\text{-}dC)_2$ with the same gradient system, the tetramer mobility was faster and distinctly separate from that of the hexamer. The chromatographic profile for $(dG\text{-}dC)_3$ under these conditions is available in the microfilm edition.

The circular dichroism spectrum was calculated by using the nearest-neighbor approximation (Cantor & Tinoco, 1965) and is in good agreement with the experimental spectrum at 80 °C. The extinction coefficients used at 20 °C were $2.95 \times 10^4$ $M^{-1}$ (strands) $cm^{-1}$ at 280 nm and $5.31 \times 10^4$ $M^{-1}$ (strands) $cm^{-1}$ at 260 nm [F. M. Pohl, personal communication; Kastrup et al. (1978)]. The extinction coefficient at 3 °C was determined from the absorbance of 10 samples ranging from $8 \times 10^{-6}$ to $1.7 \times 10^{-4}$ M at 3 and 20 °C by using $\epsilon_{3°C} = \epsilon_{20°C} A_{3°C}/A_{20°C}$. The value obtained is $2.88 \times 10^4$ $M^{-1}$ (strands) $cm^{-1}$. All melting curves were measured at 280 nm.

The effect of $D_2O$ on the extinction coefficient at 280 nm and 3 °C was determined by taking a $D_2O$ sample with an absorbance of 1.5 $cm^{-1}$, diluting it by weight with $H_2O$ buffer to 90.2 vol % $H_2O$, and remeasuring the absorbance. No change in extinction was observed, and we therefore assume there would be no change in going to 100% $H_2O$.

*Solvents.* $H_2O$ was doubly distilled in glass and deionized. $D_2O$ (99.7%) was purchased from Aldrich Chemical Co. All buffers were made up by a 100:1 dilution of a 4.5 M cacodylate solution in $H_2O$ at pH 7.7 using 1.0 M NaCl in $H_2O$ or $D_2O$. The final pH reading using a Sigma glass calomel electrode was 7.0–7.2 in $H_2O$ and 7.3–7.6 in $D_2O$.

*Spectra.* Absorption spectra and absorbance vs. temperature profiles were measured on a Gilford 250 spectrophotometer interfaced to a PDP 11/34 computer for data collection and analysis. The temperature was incremented at a rate of 30

† From the Department of Chemistry, University of Rochester, Rochester, New York 14627 (D.D.A. and D.H.T.), and the Department of Chemistry, Douglass College, Rutgers University, New Brunswick, New Jersey 08903 (L.M. and K.J.B.). *Received June 19, 1980.* This work was supported by National Institutes of Health Grants GM 22939 and GM 23509. D.H.T. is an Alfred P. Sloan Fellow.

0006-2960/81/0420-1409$01.25/0 

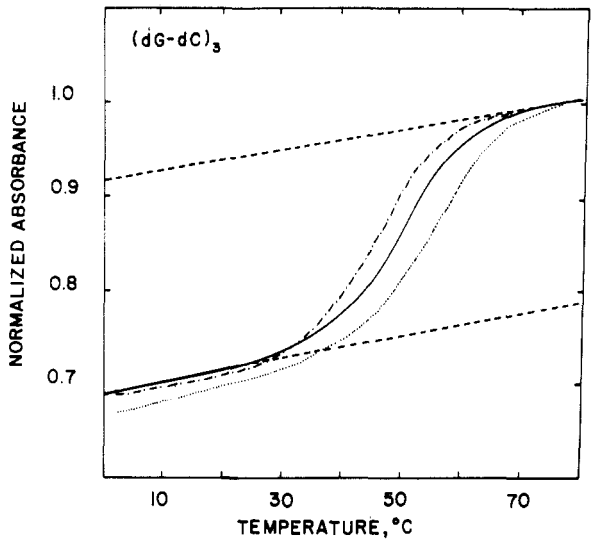


FIGURE 1: Normalized absorbance vs. temperature for $(dG\text{-}dC)_3$ in $H_2O$ at 8.5 $\mu$M (-·-), 29.1 $\mu$M (—), 131.0 $\mu$M (···). The measured absorbances for $H_2O$ are 0.366, 1.245, and 5.88/cm, respectively, at 80 °C. All solutions contain 1.0 M NaCl and 45 mM cacodylate, pH 7. The base lines shown (---) were subtracted to generate the experimental curve in Figure 2.

°C/h by using a Haake FK2 circulating bath with a programmable attachment. The temperature was monitored with a YSI 44018 thermistor placed in the reference cell. Over 340 data points were collected and analyzed for each melting curve. No corrections were made for volume expansion. This allows the results to be directly compared with those obtained with solvent mixtures (Albergo & Turner, 1981).

*Calorimetry.* The differential scanning calorimetry was carried out on a Microcal-1 instrument. In a typical experiment, the reaction and the reference platinum cells are each filled with 0.9 mL of solution, and the temperature is scanned from 5 to 95 °C at a rate of 0.92 °C/min. For a thermally induced endothermic transition, the temperature of the reaction cell will lag behind that of the solvent reference cell. In a given experiment, the additional electrical energy fed back to the reaction cell to maintain it at the same temperature as the solvent reference cell is measured continuously. The instrument is calibrated by measuring the area produced by a controlled electrical pulse. These data (along with the known concentration of the solute) permit the construction of enthalpy per mole vs. temperature and specific heat vs. temperature curves.

The concentration of the oligomer was spectrophotometrically determined by measuring the absorbance at 260 nm. The solutions used for the calorimetric experiments had concentrations of $1.03 \times 10^{-3}$ M in strands for the $H_2O$ transitions and $1.13 \times 10^{-3}$ M in strands for the $D_2O$ transitions.

## Results

Typical absorbance vs. temperature curves for $(dG\text{-}dC)_3$ are shown in Figure 1. The curves are characterized by a highly cooperative melting transition with relatively linear "base line" regions at lower and higher temperatures. The cooperative transition is assumed to reflect the coil to helix equilibrium:

$$2(dG\text{-}dC)_3 \rightleftarrows [(dG\text{-}dC)_3]_2 \quad (1)$$

The equilibrium constant, $K$, is given by

$$K = \frac{f}{2(1-f)^2 c_T} \quad (2)$$

where $c_T$ is the total strand concentration and $f$ is the fraction of strands in double helix. This two-state model was used to analyze the data in the following four ways.

(*1*) *Ln K vs. 1/T.* A plot of ln $K$ vs. $1/T$ yields the enthalpy, $\Delta H$, and the entropy, $\Delta S$, from the slope and intercept, respectively:

$$\ln K = -\frac{\Delta H}{R}\frac{1}{T} + \frac{\Delta S}{R} \quad (3)$$

Determination of $K$ at each temperature requires the calculation of the respective $f$'s (see eq 2). These can be calculated by using

$$f = \frac{c_T \epsilon_s(T) - A(T)}{c_T \epsilon_s(T) - \frac{c_T}{2}\epsilon_d(T)} \quad (4)$$

where $A(T)$ is the absorbance and $\epsilon_s(T)$ and $\epsilon_d(T)$ are the extinctions of the single strand and double helix, respectively. Use of eq 4 requires knowledge of the initial- and final-state extinction coefficients. Three conventions have been used to estimate these quantities.

(*a*) *Limiting Values.* In this case the extinction coefficients of the initial and final states are taken as those measured at the lowest and highest temperatures, respectively. The corresponding states are presumably close to the fully bonded double helix and the unstacked single strand. Unfortunately, this treatment results in curved ln $K$ vs. $1/T$ plots. Such curvature can be caused by a temperature-dependent enthalpy and/or the presence of more than two states.

(*b*) *Subtracting Upper Base Line.* In this case, the high-temperature linear region of the melting curve is used to define a linear temperature-dependent extinction coefficient for the final state (Martin et al., 1971). The major reason for this slope is the equilibrium between single-strand stacked and unstacked species. Thus, the final state in this analysis is a partially stacked single strand (Pörschke et al., 1973).

(*c*) *Subtracting Upper and Lower Base Lines.* In this case, the low- and high-temperature linear base lines are used to define temperature-dependent extinction coefficients for the initial and final states, respectively. This introduces a temperature-dependent double-helical state as the initial state. The nature of this intramolecular equilibrium has not been determined. Two candidates are unpairing (fraying) of terminal base pairs or species containing less than six base pairs (Patel, 1976; Borer et al., 1975).

Once the limiting extinction coefficients have been chosen, $f$ is calculated with eq 4. These $f$ values can then be used in eq 2 to calculate $K$ as a function of temperature. Then the enthalpy and entropy are computed from eq 3.

(*2*) *Slope at $T_m$.* Once $f$ values have been computed as described above, the enthalpy can be calculated from

$$\Delta H = 6RT_m^2\left(\frac{df}{dT}\right)_{T_m} \quad (5)$$

where $df/dT$ is taken at the temperature, $T_m$, where $f = 0.5$.

(*3*) *Shape Analysis.* The absorbance vs. temperature curves can be fit to eq 2, 3, and 4 with a nonlinear least-squares program (Bevington, 1969). The parameters fitted are $\Delta H$, $\Delta S$, $\epsilon_s$, $\epsilon_d$, and $c_T$. The program was tested with ideal two-state data with and without random error. In each case the program converged to the parameters used to generate the data within the calculated standard deviation. These deviations were typically ±1% for $\Delta H$ and $\Delta S$ and ±0.5% for $\epsilon_s$, $\epsilon_d$, and $c_T$ for a random error in the data of 0.5%. When raw absorbance data (e.g., Figure 1) were used, the fitted curve deviated substantially from the measured curve, again indicating the presence of more than two states and/or a temperature-de-

Table I: Calorimetric and Spectroscopic Enthalpies for Coil to Helix Transition in $(dG\text{-}dC)_3$ (kcal/mol)

| | shape analysis | | | $1/T$ vs. log $c_T$ | | |
|---|---|---|---|---|---|---|
| | ln $K$ vs. $1/T$ | slope at $T_m$ | nonlinear | $1/T_m$ | $1/T_{max}$ | calorimetry |
| no base line subtracted | −39.0 | −42.1 | −33.0 | −58.1 | −56.6 (−66.6) | |
| upper base line subtracted | −37.0 | −41.4 | | −57.6 | | |
| both base lines subtracted | −58.9 | −56.8 | −56.6 (−59.7) | −57.4 (−61.8) | | −59.6 (−65.8) |

Table II: Entropies for Coil to Helix Transition in $(dG\text{-}dC)_3$ [cal/(mol deg)]

| | shape analysis | | | $1/T$ vs. log $c_T$ | |
|---|---|---|---|---|---|
| | ln $K$ vs. $1/T$ | slope at $T_m$ | nonlinear | $1/T_m$ | $1/T_{max}$ |
| no base line subtracted | −101.3 | −110.8 | −84.0 | −160.3 | −154.2 (−184.1) |
| upper base line subtracted | −95.4 | −100.0 | | −152.0 | |
| both base lines subtracted | −162.2 | −155.6 | −154.9 (−164.1) | −157.4 (−171.1) | |

pendent enthalpy. This was also true if a sloping upper base line was subtracted from the data before fitting. However, if both a lower and an upper base line were subtracted, excellent fits were obtained. A typical curve analyzed in this manner is shown in Figure 2.

*(4) $1/T_m$ vs. Log $c_T$.* A plot of $1/T_m$ vs. log $c_T$ gives $\Delta H$ and $\Delta S$ from the slope and intercept, respectively (Borer et al., 1974):

$$\frac{1}{T_m} = \frac{2.3R}{\Delta H} \log c_T + \frac{\Delta S}{\Delta H} \qquad (6)$$

The $T_m$'s are obtained from $f$ vs. $T$ curves generated after subtraction of upper and lower base lines. Plots are shown in Figure 3. A modification of method 4 is to take the derivative of the absorbance vs. $T$ curves with respect to reciprocal temperature ($dA/dT^{-1}$) (without base line subtraction) and plot inverse temperature at the maximum derivative, $1/T_{max}$, as a function of log $c_T$ (see Figure 4). Assuming $T_{max}$ corresponds to the temperature at which $f = 0.41$ (Gralla & Crothers, 1973), the thermodynamics are then derived from

$$\frac{1}{T_{max}} = \frac{2.3R}{\Delta H} \log c_T + \frac{(\Delta S + 0.529R)}{\Delta H} \qquad (7)$$

In practice, the noise in the melting curves makes this method unusable unless some smoothing is applied. Calculations with ideal two-state data containing 0.5 or 1.0% random error indicated that a quadratic fit with a smoothing interval of 12–14 °C was optimal. Thus, derivative curves were obtained by taking a least-squares interwoven 60–70-point fit to a quadratic and computing the analytical derivative (Bevington, 1969). Typical deviations between calculated and experimental curves range from 0.1 to 0.7%. Plots of $1/T_{max}$ vs. log $c_T$ determined in this manner are shown in Figure 4. The advantage of this analysis is that it does not require knowledge of the initial- and final-state extinction coefficients. The implicit assumption is the inflection point for each concentration in a given solvent corresponds to the same thermodynamic state.

The thermodynamics derived from the above analyses are listed in Tables I and II. All methods were used on $H_2O$ data, but only the three considered most reliable were used for $D_2O$. These latter results are listed in parentheses.

The calorimetric values for the enthalpies were determined by integration of heat capacity curves. Figure 5 shows a tracing of an actual calorimetric scan between 15 and 95 °C with associated buffer base line. Figure 6 shows the heat

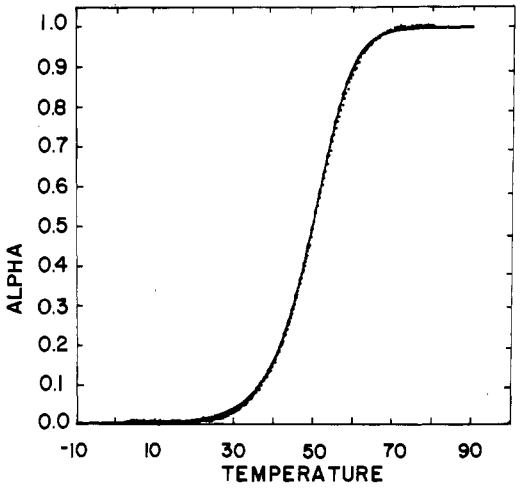


FIGURE 2: $\alpha$ vs. temperature for $(dG\text{-}dC)_3$ showing (···) the experimental curve after subtracting upper and lower base lines and (—) the nonlinear two-state fit to the data. The strand concentration is 29.1 $\mu$M in $H_2O$ containing 1.0 M NaCl and 45 mM cacodylate, pH 7. $\alpha$ is the fraction of oligomer in single strand and is equal to $1 - f$.

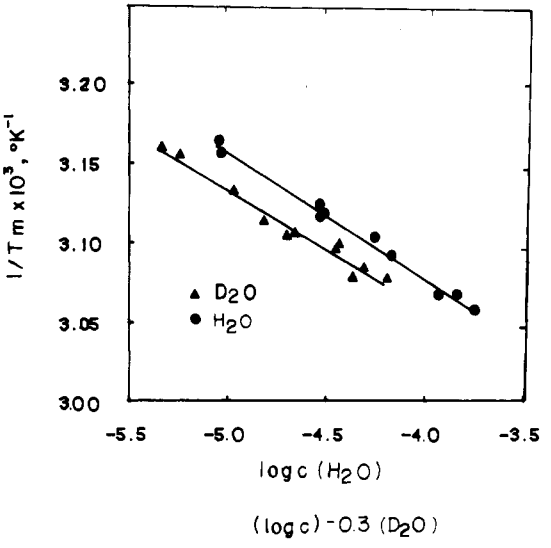


FIGURE 3: Plots of $1/T_m$ vs. log $c$ for $(dG\text{-}dC)_3$ in $H_2O$ (●) and $1/T_m$ vs. (log $c$) − 0.3 for $(dG\text{-}dC)_3$ in $D_2O$ (▲). All solutions contain 1.0 M NaCl and 45 mM cacodylate.

capacity curves obtained by averaging three such experiments. The resulting transition curves are available in the microfilm edition (see paragraph at end of paper regarding supplemen-

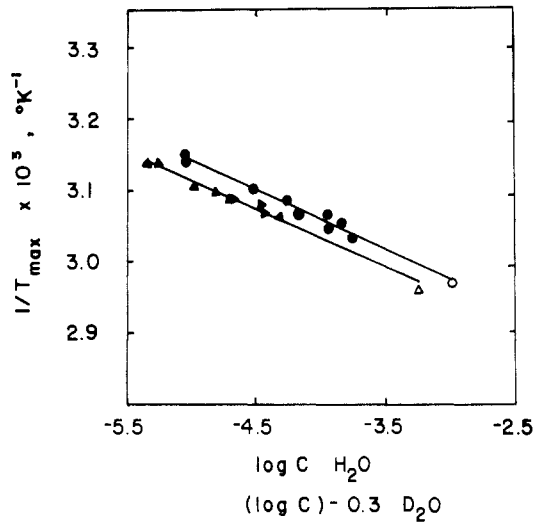


FIGURE 4: Plots of $1/T_{max}$ vs. log $c$ for $(dG\text{-}dC)_3$ in $H_2O$ (●) and $1/T_{max}$ vs. (log $c$) − 0.3 for $(dG\text{-}dC)_3$ in $D_2O$ (▲). The open circle and open triangle represent the calorimetric points for $H_2O$ and $D_2O$, respectively. All solutions contain 1.0 M NaCl and 45 mM cacodylate.

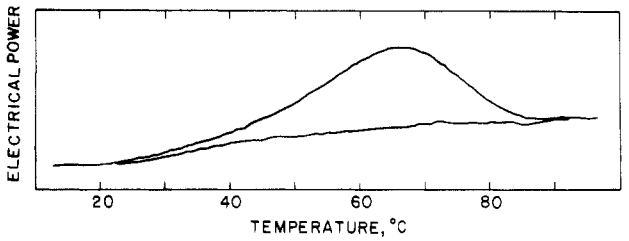


FIGURE 5: Electrical power (fed back to sample cell to maintain it at same temperature as reference cell) vs. temperature. Figure shown is tracing of recorder output obtained from a single scan in water. For upper curve, sample cell contained $1.03 \times 10^{-3}$ M $(dG\text{-}dC)_3$ in 1.0 M NaCl, 45 mM cacodylate, pH 7, and $H_2O$. For lower curve both cells contained only buffer.

tary material). The enthalpies determined are listed in Table I. For each transition, the solution was cooled down and scanned a second time. All repeat scans resulted in essentially superimposable heat capacity curves. This observation allows us to conclude that the transitions are completely reversible.

## Discussion

The main purpose of this work is to compare enthalpies determined spectroscopically and calorimetrically in order to suggest judicious methods for analyzing spectroscopic data. The results in Table I show that with $(dG\text{-}dC)_3$ all four methods give good agreement with calorimetry when both an upper and lower base line are subtracted before analysis. If base lines are not subtracted, only $1/T$ vs. log $c_T$ plots provide reasonable concordance. The $1/T$ vs. log $c_T$ results are insensitive to base line manipulation. Comparison of results for the much different oligomer $rA_7U_7$ shows similar agreement between calorimetric and $1/T$ vs. log $c_T$ derived enthalpies (Breslauer et al., 1975; Martin et al., 1971). The enthalpies derived from the spectroscopic analyses described above are all based on a two-state model. These values will only agree with the model independent calorimetric enthalpy if the latter is dominated by the enthalpy of the cooperative helix to coil transition of eq 1. The close congruence of results suggests this bimolecular process does dominate.

Using eq 6, Pohl reports a $\Delta H$ of −50.9 kcal/mol for the helix to coil transition of an approximately equal mixture of $(dG\text{-}dC)_3$ and $(dC\text{-}dG)_3$ (Pohl, 1974). This is in reasonable agreement with the value of −57.4 kcal/mol obtained by sim-

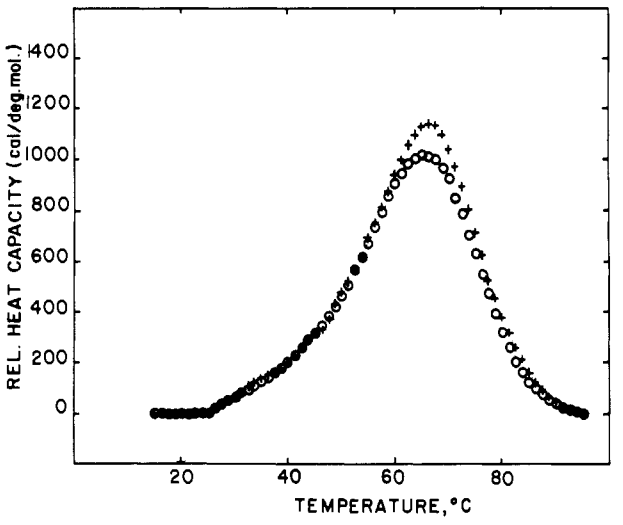


FIGURE 6: Calorimetric heat capacity vs. temperature for $(dG\text{-}dC)_3$ in $H_2O$ (○) and $D_2O$ (+). The strand concentration is $1.03 \times 10^{-3}$ M in $H_2O$ and $1.13 \times 10^{-3}$ M in $D_2O$ containing 1.0 M NaCl and 45 mM cacodylate. Both curves are averages of three runs.

ilar analysis in this work. The calorimetric value for $\Delta H$ is −59.6 kcal/mol. If the first base pair is assumed to have a $\Delta H$ of 0, this corresponds to an average $\Delta H$ of −11.9 kcal/mol of stack (Borer et al., 1974). This is somewhat lower than the average of −13.8 kcal/mol of stack found for GC and CG sequences in ribooligomers (Borer et al., 1974).

An interesting aspect of the results in Table I is that the enthalpy for helix formation of $(dG\text{-}dC)_3$ is ~10% more favorable in $D_2O$ than in $H_2O$, and the entropy is ~15% less favorable. Thus the relative stability of the helix in $H_2O$ and $D_2O$ will depend on the temperature. One consequence is that caution must be used when comparing melting temperatures derived from NMR experiments in $D_2O$ with those obtained spectroscopically in $H_2O$. The results suggest that hydrogen bonding and bound water may be important factors in formation of the $(dG\text{-}dC)_3$ double helix. A previous calorimetric study with poly(A)–poly(U) indicated no difference in enthalpy between $H_2O$ and $D_2O$ (Klump, 1972). Of course, these two systems have very different characteristics. We are pursuing work on additional double helices in order to understand these effects.

## Acknowledgments

We thank M. Petersheim for writing the nonlinear fitting program.

## Supplementary Material Available

One figure showing the high-pressure liquid chromatogram of $(dG\text{-}dC)_3$ and two figures showing calorimetric transition curves (3 pages). Ordering information is given on any current masthead page.

## References

Albergo, D. D., & Turner, D. H. (1981) *Biochemistry* (second of three papers in this issue).

Bevington, P. R. (1969) *Data Reduction and Error Analysis for the Physical Sciences*, McGraw-Hill, New York.

Borer, P. N., Dengler, B., Uhlenbeck, O. C., & Tinoco, I. (1974) *J. Mol. Biol. 86*, 843.

Borer, P. N., Kan, L. S., & Ts'o, P. O. P. (1975) *Biochemistry 14*, 4847.

Breslauer, K. J., Sturtevant, J. M., & Tinoco, I. (1975) *J. Mol. Biol. 99*, 549.

Cantor, C. R., & Tinoco, I. (1965) *J. Mol. Biol. 13*, 65.

Gralla, J., & Crothers, D. M. (1973) J. Mol. Biol. 78, 301.
Kastrup, R. V., Young, M. A., & Krugh, T. R. (1978) Biochemistry 17, 4855.
Klump, H. (1972) Biopolymers 11, 2331.
Martin, F. H., Uhlenbeck, O. C., & Doty, P. (1971) J. Mol. Biol. 57, 201.
Patel, D. J. (1976) Biopolymers 15, 533.
Pohl, F. M. (1974) Eur. J. Biochem. 42, 495.
Pörschke, D., Uhlenbeck, O. C., & Martin, F. H. (1973) Biopolymers 12, 1313.

# Solvent Effects on Thermodynamics of Double-Helix Formation in $(dG\text{-}dC)_3$†

Diane DePrisco Albergo and Douglas H. Turner*

ABSTRACT: The thermodynamics of double-helix formation by $(dG\text{-}dC)_3$ have been measured in aqueous solvent mixtures containing 10 mol % methanol, ethanol, 1-propanol, formamide, *N*,*N*-dimethylformamide, or urea and 20 mol % ethanol. Optical activity measurements indicate the conformation of the double helix at 3 °C is the same in all the solvent mixtures except 20 mol % ethanol. All the cosolvents destabilize the helix relative to water. With 10 mol % alcohol cosolvents, this destabilization is associated with a more unfavorable entropy change averaging ~8% and a more favorable enthalpy change averaging ~5%. This is consistent with a small contribution of hydrophobic bonding to stability. In contrast, the destabilization by formamide, *N*,*N*-dimethylformamide, and urea is associated with a more unfavorable enthalpy change averaging ~23% and a more favorable entropy change averaging ~21%. Since all three of these cosolvents have dipole moments larger than water, this is consistent with increased competition for dipolar interactions between the nucleic acid bases. None of the results correlate with any one bulk solvent parameter such as surface tension, viscosity, or dielectric constant. With 20 mol % ethanol, optical activity measurements are consistent with a partial B to C form transition. This is associated with a 27% less favorable enthalpy and 25% more favorable entropy for helix formation relative to water. Since the B to C transition is associated with helix dehydration, this may imply a significant contribution of bound water to stability.

It has been suggested that solvent plays an important role in the conformational stability of nucleic acids (T'so et al., 1969; Levine et al., 1963; Lowe & Schellman, 1972; Breslauer et al., 1978; Girod et al., 1973; Cantor & Schimmel, 1980). However, there is debate over the mechanism involved. The denaturation of deoxyribonucleic acid (DNA) by alcohols initially implicated hydrophobic interactions (Herskovits, 1963). However, the helix was subsequently shown to be stabilized by a favorable enthalpy, whereas hydrophobic bonding is associated with a favorable entropy (Kauzmann, 1959; Tanford, 1973). The only theory of solvent participation that qualitatively predicts the correct thermodynamics suggests the energy of cavity formation plays a dominant role (Sinanoglu & Abdulnur, 1964, 1965; Abdulnur, 1966; Sinanoglu, 1968). This has been called "solvophobic" bonding. Although the theory is in qualitative agreement with trends in denaturation by mixed solvents, it has never been thoroughly tested. The only parameter that has been quantitatively correlated with the degree of destabilization of DNA is solubility (Herskovits & Harrington, 1972; Herskovits & Bowen, 1974; Levine et al., 1963).

The availability of oligonucleotides of defined length and sequence provides the opportunity for a more detailed investigation of the role of solvent. This paper reports the thermodynamics associated with the coil to helix transition of the deoxyhexanucleotide $(dG\text{-}dC)_3$ in mixed aqueous solvent systems. Previous studies have characterized this transition in $H_2O$ and $D_2O$ (Pohl, 1974; Albergo et al., 1981).

## Experimental Procedures

*Oligonucleotide.* d-GpCpGpCpGpC was purchased from Collaborative Research. Tests for purity and the extinction coefficients used are described in the preceding paper (Albergo et al., 1981). The effect of solvent on the extinction coefficient at 280 nm at 3 °C was determined by measuring the absorbance of a concentrated sample in the solvent mixture (e.g., 10 mol % EtOH),[1] diluting it by 10 with water buffer, and remeasuring the absorbance. No change in extinction at 280 nm was observed for the solvents used here.

*Solvents.* Formamide was purified by recrystallization (Casey & Davidson, 1977). The absorbance at 270 nm was 0.07/cm. Spectral grade *N*,*N*-dimethylformamide was from Mallinckrodt. The absorbance was 0.28/cm at 275 nm. Water was double-distilled, and absolute ethanol was used. Methanol was spectral grade from Mallinckrodt, 1-propanol "distilled in glass" was from Burdick and Jackson, and urea was "ultra pure" from Schwarz/Mann.

All solvents were checked for purity by index of refraction and NMR. Water and alcohol solvents were checked for cation content by Eriochrome Black T–EDTA titration. The cation concentration was below the detection limit of $10^{-6}$ M in all cases. Solutions were made by diluting a 4.5 M caco-

† From the Department of Chemistry, University of Rochester, Rochester, New York 14627. *Received June 19, 1980.* This work was supported by National Institutes of Health Grant 22939. D.H.T. is an Alfred P. Sloan Fellow.

[1] Abbreviations used: MeOH, methanol; EtOH, ethanol; PrOH, 1-propanol; DMF, *N*,*N*-dimethylformamide; CD, circular dichroism; CMP, cytidine monophosphate; EDTA, ethylenediaminetetraacetic acid.

0006-2960/81/0420-1413$01.25/0 